

Non-Markovian quantum state diffusion for absorption spectra of molecular aggregates

Jan Roden,¹ Walter T. Strunz,² and Alexander Eisfeld^{1,*}

¹*Max-Planck-Institut für Physik komplexer Systeme, Nöthnitzer Str. 38, D-01187 Dresden, Germany*

²*Institut für Theoretische Physik, Technische Universität Dresden, D-01062 Dresden, Germany*

(Dated: August 4, 2018)

In many molecular systems one encounters the situation where electronic excitations couple to a quasi-continuum of phonon modes. That continuum may be highly structured e.g. due to some weakly damped high frequency modes. To handle such a situation, an approach combining the non-Markovian quantum state diffusion (NMQSD) description of open quantum systems with an efficient but abstract approximation was recently applied to calculate energy transfer and absorption spectra of molecular aggregates [Roden, Eisfeld, Wolff, Strunz, PRL 103 (2009) 058301]. To explore the validity of the used approximation for such complicated systems, in the present work we compare the calculated (approximative) absorption spectra with exact results. These are obtained from the method of pseudomodes, which we show to be capable of determining the exact spectra for small aggregates and a few pseudomodes. It turns out that in the cases considered, the results of the two approaches mostly agree quite well. The advantages and disadvantages of the two approaches are discussed.

I. INTRODUCTION

There is growing interest in systems composed of individual monomers that interact via resonant dipole-dipole interaction. Upon electronic excitation this transition dipole-dipole interaction between the monomers is responsible for a collective behaviour of these systems. Besides the classical examples like Van-der-Waals crystals [1, 2], aggregates of organic dyes [3–7], and light harvesting units of plants, algae, and bacteria [6, 8–11] many new systems have emerged. Examples are ultra-cold Rydberg atoms [12–16], quantum dots [17, 18], assemblies of nano-particles [19, 20], and recently also hybrid systems [21].

The common approach to describe these aggregates is to treat the monomers as electronic two-level systems. Besides the electronic degrees of freedom, however, one often has to take into account nuclear degrees of freedom explicitly. For instance in the case of molecular aggregates [7, 22–26], which will serve as the primary example in this work, the electronic excitation of a monomer couples strongly to internal vibrational modes of the monomer and to modes of the surroundings.

Often, the monomer spectrum is dominated by one vibrational progression which is considerably broadened. A commonly applied approximation is then to only consider one effective mode corresponding to this progression [27, 28] and to take the broadening into account by convoluting with some lineshape function which is usually assumed to be Gaussian. It has been shown that using this approach already important features of experimental spectra can be reproduced [28–33]. Although the resulting spectra reveal many characteristics of the aggregates, important aspects like the detailed shapes of

the J-band [34] and the H-band [35] cannot adequately be described by considering only one vibrational mode. On the other hand, the exact inclusion of only *one* vibrational mode already complicates the treatment of molecular aggregates considerably, so that this approach is restricted to small aggregates. This problem becomes even more serious when one attempts to include more modes in this manner.

When the interaction of the chromophore monomers with the environment is negligible (e.g. in high resolution spectroscopy in helium nanodroplets [24, 36]), then the *explicit* inclusion of vibrational modes is of great importance. However, for typical spectra in solution or in a solid state matrix (where a strong coupling between the chromophores and the environment is present) it seems better to use a continuum of vibrations that couple to the electronic excitation to account for the large number of environmental degrees of freedom.

This interaction between the electronic excitation and the vibrations is conveniently encoded in the so-called spectral density. It describes the frequency-dependent coupling between the system (the electronic degrees of freedom) and the (continuum of) harmonic oscillators. In the Markov case the spectral density is assumed to be flat in the relevant frequency regions. Clearly, for the considered monomers this assumption does not hold. Due to strong interaction with some internal vibrational modes, the spectral density will be highly structured (i.e. frequency-dependent), indicating that a non-Markovian theoretical framework is required.

An approach to tackle this complicated problem was recently presented in Ref [37]. The method is based on the non-Markovian quantum state diffusion (NMQSD) description of open quantum systems [38]. Here, the system part is chosen to contain only the electronic degrees of freedom which interact with a non-Markovian environment (the bath) comprising all vibrations (internal modes of the monomers as well as external modes). One

*Electronic address: eisfeld@mpiiks-dresden.mpg.de

then can derive a stochastic evolution equation for states in the (small) space of the system part. However, solving the exact evolution equation turns out to be very difficult due to the appearance of a functional derivative w.r.t. functionals containing the bath degrees of freedom. To overcome these difficulties, in an approximation only the zeroth order of a functional expansion (we will refer to it as ZOFE approximation) of the problematic term is taken into account [37, 39]. For several (simple) problems this procedure has been shown to give the exact result [40, 41]. However, for more complex problems like the molecular aggregates studied in this work, the range of validity of the approximation is not clear. It should be noted that the NMQSD approach in combination with the ZOFE approximation provides a very efficient calculation scheme: in order to obtain the absorption spectrum of the aggregate and the energy transfer between the monomers, the equations one has to solve are in the small Hilbert space of the electronic degrees of freedom alone [37].

One aim of the present paper is to examine the validity of the ZOFE approximation leading to the calculation scheme presented in Ref. [37]. To this end, we compare with an approach where so-called pseudomodes [42–44] are included into the system part together with the electronic degrees of freedom. The electronic degrees of freedom now couple only to the pseudomodes, the pseudomodes in turn are then coupled to a Markovian bath. For a spectral density consisting of a sum of Lorentzians the pseudomode method is exact (taking one pseudomode for each Lorentzian). This allows to directly compare the approximative NMQSD-ZOFE treatment with exact calculations. However, due to the inclusion of the pseudomodes into the system part, the numerical solution of the corresponding evolution equation is limited to a rather small number of monomers in the aggregate with only a few pseudomodes, i.e. only a few Lorentzians in the spectral density.

Besides the possibility of comparing the NMQSD-ZOFE approach with exact calculations, the pseudomode method has also some physical significance: one can think of the pseudomodes as internal vibrational modes of a chromophore that strongly couple to the electronic excitation and which are damped by the coupling to the remaining vibrations.

The comparison between zero temperature absorption spectra of small aggregates calculated using the NMQSD-ZOFE approach and spectra obtained from the exact pseudomode approach shows that in the cases considered there is mostly quite good agreement between the two approaches. We will discuss in which situations the approximative result of the NMQSD-ZOFE approach is expected to deviate from the exact solution.

The structure of this paper is as follows: In Section II, we introduce the Hamiltonian of the aggregate. The Hamiltonian is written as the sum of a system part (containing only electronic degrees of freedom), an environmental part (containing all vibrational modes), and the

part of the interaction between electronic degrees of freedom and vibrations. In the following Section III, the basic formulas that are used to calculate the absorption spectrum are given by specifying the initial state and introducing the dipole correlation function. In Section IV, the general Non-Markovian Schrödinger Equation (NMQSD) approach is applied to the case of an aggregate. It is shown how the absorption spectrum can be obtained in this approach. Next, in Section V, the ZOFE approximation is introduced. Then, in Section VI, the pseudomode (PM) approach is presented. In Section VII, the NMQSD-ZOFE absorption spectra are compared with exact PM spectra. We conclude in Section VIII by summarizing our findings. Details of the calculations and minor results have been placed in the appendices. In Appendix A, two exactly solvable cases (namely that of non-interacting monomers and the case where the coupling to the vibrations can be considered to be Markovian) are discussed. In Appendix B, it is shown how to obtain the absorption spectrum using the PM approach. The numerical implementation is discussed. Finally, in Appendix C, it is shown that for a Lorentzian spectral density the absorption spectrum obtained from the exact NMQSD approach is equal to the spectrum obtained from the PM method.

II. THE AGGREGATE HAMILTONIAN

We consider an aggregate consisting of N monomers, labelled by $n = 1, \dots, N$. For each monomer n we take into account its electronic ground state $|\phi_n^g\rangle$ and one excited electronic state $|\phi_n^e\rangle$. The transition energy between these two states (whose wave functions we take to be real) is denoted by ε_n . Apart from the two electronic states, each monomer has a collection of vibrational modes comprising internal modes as well as modes of the local environment of the monomer. We will refer to these degrees of freedom as “nuclear coordinates”. The electronic excitation of monomer n couples to its vibrations and we choose the vibrational modes to be harmonic and the coupling to be linear (making contact to previous work [29, 30, 45–50]). The Hamiltonian of monomer n is then given by

$$H_n = H_n^g |\phi_n^g\rangle \langle \phi_n^g| + H_n^e |\phi_n^e\rangle \langle \phi_n^e|, \quad (1)$$

with the Hamiltonian of the vibrations in the electronic ground state

$$H_n^g = \sum_{\lambda} \hbar \omega_{n\lambda} a_{n\lambda}^{\dagger} a_{n\lambda} \quad (2)$$

(the energies of the vibrational ground states of all modes in the electronic ground state are chosen to be zero). The Hamiltonian of the vibrations in the excited electronic state comprising a shift, reads

$$H_n^e = \varepsilon_n + \sum_{\lambda} \hbar \omega_{n\lambda} a_{n\lambda}^{\dagger} a_{n\lambda} - \sum_{\lambda} \kappa_{n\lambda} (a_{n\lambda}^{\dagger} + a_{n\lambda}). \quad (3)$$

Here $a_{n\lambda}$ denotes the annihilation operator of mode λ of monomer n with frequency $\omega_{n\lambda}$. The coupling strength with which electronic excitation of monomer n couples to mode λ of this monomer is denoted by $\kappa_{n\lambda}$.

For the aggregate we assume that the electronic wave functions of the monomers do not overlap. The electronic ground state of the aggregate is then taken as the product

$$|g_{\text{el}}\rangle = \prod_{m=1}^N |\phi_m^g\rangle \quad (4)$$

of the electronic ground states $|\phi_m^g\rangle$ of all monomers. A state of the aggregate in which only monomer n is electronically excited and all other monomers are in their electronic ground state we denote by

$$|\pi_n\rangle = |\phi_n^e\rangle \prod_{m \neq n} |\phi_m^g\rangle. \quad (5)$$

We expand the aggregate Hamiltonian w.r.t. the states Eqs. (4) and (5) and neglect states with more than one electronic excitation on the aggregate. Thus we obtain the Hamiltonian

$$H = H^g |g_{\text{el}}\rangle \langle g_{\text{el}}| + H^e \sum_{n=1}^N |\pi_n\rangle \langle \pi_n| \quad (6)$$

for the aggregate, with the part

$$H^g = \sum_{n=1}^N H_n^g \quad (7)$$

for the electronic ground state and the part

$$H^e = \sum_{n=1}^N \left(H_n^e + \sum_{m \neq n}^N H_m^g \right) |\pi_n\rangle \langle \pi_n| + \sum_{n,m=1}^N V_{nm} |\pi_n\rangle \langle \pi_m| \quad (8)$$

for the electronically excited state. The matrix element V_{nm} , causing electronic excitation to be transferred from monomer n to monomer m via transition dipole-dipole interaction, is taken to be independent of nuclear coordinates (note that H_n^g and H_n^e depend on nuclear coordinates through Eqs. (2) and (3)). With the Hamiltonians of the monomers Eqs. (2) and (3) we can write Eq. (8) as

$$H^e = H_{\text{sys}} + H_{\text{int}} + H_{\text{env}}, \quad (9)$$

with the purely electronic ‘‘system’’ part

$$H_{\text{sys}} = \sum_{n=1}^N \varepsilon_n |\pi_n\rangle \langle \pi_n| + \sum_{n,m=1}^N V_{nm} |\pi_n\rangle \langle \pi_m|, \quad (10)$$

and a part H_{env} describing the ‘‘environment’’ of vibrational modes

$$H_{\text{env}} = \sum_{n=1}^N \sum_{\lambda} \hbar \omega_{n\lambda} a_{n\lambda}^\dagger a_{n\lambda}. \quad (11)$$

The coupling of electronic excitation to these vibrations is expressed through

$$H_{\text{int}} = - \sum_{n=1}^N |\pi_n\rangle \langle \pi_n| \sum_{\lambda} \kappa_{n\lambda} (a_{n\lambda}^\dagger + a_{n\lambda}). \quad (12)$$

We emphasize that with Eqs. (10)-(12) we make a special choice of the three parts, system, interaction and environment, of the aggregate Hamiltonian. In particular the system part Eq. (10) contains only electronic degrees of freedom. In Section VI, where we will introduce the pseudomode approach, we will include also vibrational modes (pseudomodes) into the system part.

A useful quantity describing many aspects of the coupling of the system degrees of freedom to the vibrational environment is the so-called spectral density [51], which for monomer n is given by

$$J_n(\omega) = \sum_{\lambda} |\kappa_{n\lambda}|^2 \delta(\omega - \omega_{n\lambda}) \quad (13)$$

and which will be used later, generalized to a continuum of vibrational modes.

III. ABSORPTION OF THE AGGREGATE

We consider absorption of light by the aggregate at zero temperature. Initially, the aggregate is taken to be in its total ground state

$$|\Phi(t=0)\rangle = |g_{\text{el}}\rangle |0\rangle, \quad (14)$$

which is a product of the electronic ground state $|g_{\text{el}}\rangle$ defined in Eq. (4) and the ground state $|0\rangle = \prod_{n\lambda} |0_{n\lambda}\rangle$ of H_{env} , i.e. all vibrational modes of all monomers are in their ground state $|0_{n\lambda}\rangle$. The absorption of light with frequency ν and polarization $\vec{\mathcal{E}}$ is then given by [51]

$$A(\nu) = \text{Re} \int_0^\infty dt e^{i\nu t} M(t). \quad (15)$$

Here,

$$M(t) = \langle \Phi(t=0) | \hat{\vec{\mu}} \cdot \vec{\mathcal{E}} e^{-iHt/\hbar} \hat{\vec{\mu}} \cdot \vec{\mathcal{E}}^* | \Phi(t=0) \rangle \quad (16)$$

is the dipole correlation function where $\hat{\vec{\mu}}$ denotes the total dipole operator of the aggregate, given by the sum

$$\hat{\vec{\mu}} = \sum_{n=1}^N \hat{\vec{\mu}}_n \quad (17)$$

of all monomer dipole operators $\hat{\mu}_n$. Note that the Hamiltonian H in the exponent of the propagator in Eq. (16) is the aggregate Hamiltonian of Eq. (6). We take $\hat{\mu}_n$ to be independent of nuclear coordinates. Then the correlation function Eq. (16) with Eq. (14) reads

$$M(t) = \sum_{n,m=1}^N (\vec{\mu}_m^* \cdot \vec{\mathcal{E}}) \langle \pi_m | \langle 0 | e^{-iHt/\hbar} | 0 \rangle | \pi_n \rangle (\vec{\mu}_n \cdot \vec{\mathcal{E}}^*), \quad (18)$$

with the monomer transition dipoles

$$\vec{\mu}_n \equiv \langle \phi_n^e | \hat{\mu}_n | \phi_n^g \rangle. \quad (19)$$

Defining

$$\mu_{\text{tot}} \equiv \sqrt{\sum_{n=1}^N |\vec{\mu}_n \cdot \vec{\mathcal{E}}^*|^2}, \quad (20)$$

equation (18) can be written as

$$M(t) = \mu_{\text{tot}}^2 \langle \Psi(t=0) | \Psi(t) \rangle \quad (21)$$

with

$$|\Psi(t)\rangle = \exp(-iH^e t/\hbar) |\Psi(t=0)\rangle, \quad (22)$$

where H^e is given by Eq. (8) and the initial state is

$$|\Psi(t=0)\rangle = |\psi_0\rangle |0\rangle. \quad (23)$$

The normalized initial electronic state $|\psi_0\rangle$ in Eq. (23) is given by

$$|\psi_0\rangle = \frac{1}{\mu_{\text{tot}}} \sum_{n=1}^N (\vec{\mu}_n \cdot \vec{\mathcal{E}}^*) |\pi_n\rangle \quad (24)$$

and contains explicitly the geometry of the aggregate via the orientation of the transition dipoles $\vec{\mu}_n$ of the monomers. In the following, our goal will be to obtain the state $|\Psi(t)\rangle$ to be able to calculate the absorption spectrum according to Eqs. (15) and (21).

IV. THE GENERAL NMQSD APPROACH

The correlation function $M(t)$ of Eq. (21) can be obtained using the framework of stochastic Schrödinger equations, here the non-Markovian quantum state diffusion (NMQSD) approach (Ref. [38]). Note, however, that no stochasticity will enter in the following calculations due to the fact that for a zero temperature absorption spectrum considered in this work, one has to project on the environmental ground state (see section IV B). For energy transfer between monomers, however, the full stochasticity of the non-Markovian quantum state diffusion (NMQSD) approach (Ref. [38]) resurfaces [37].

A. NMQSD evolution equation for system states

We briefly summarize the NMQSD approach as applied to molecular aggregates. First, we transform H^e to the interaction representation w.r.t. H_{env} , yielding

$$H^e(t) = H_{\text{sys}} + \sum_{n=1}^N (L_n A_n^\dagger(t) + L_n^\dagger A_n(t)) \quad (25)$$

with

$$L_n \equiv -|\pi_n\rangle \langle \pi_n| = L_n^\dagger \quad (26)$$

and

$$A_n(t) \equiv \sum_{\lambda} \kappa_{n\lambda} a_{n\lambda} e^{-i\omega_{n\lambda} t}. \quad (27)$$

Thus, we have the time-dependent Schrödinger equation

$$i\hbar \partial_t |\Psi(t)\rangle = H^e(t) |\Psi(t)\rangle \quad (28)$$

in the interaction picture. In the next step we expand the total wave function $|\Psi(t)\rangle$ w.r.t. Bargmann coherent states $|z_{n\lambda}\rangle = \exp(z_{n\lambda} a_{n\lambda}^\dagger) |0_{n\lambda}\rangle$ [52] of the vibrations, where $|0_{n\lambda}\rangle$ is the ground state of vibrational mode λ of monomer n and the $z_{n\lambda}$ are complex numbers. One then obtains

$$|\Psi(t)\rangle = \int \frac{d^2\mathbf{z}}{\pi} e^{-|\mathbf{z}|^2} |\psi(t, \mathbf{z}^*)\rangle |\mathbf{z}\rangle, \quad (29)$$

with states $|\psi(t, \mathbf{z}^*)\rangle$ in the space of the electronic system H_{sys} , $|\mathbf{z}\rangle = \prod_n \prod_\lambda |z_{n\lambda}\rangle$, and $d^2z = d\text{Re}(z) d\text{Im}(z)$. Inserting Eq. (29) into Eq. (28) one finds [38] that the states $|\psi(t, \mathbf{z}^*)\rangle$ appearing in Eq. (29) obey an evolution equation

$$\begin{aligned} \partial_t |\psi(t, \mathbf{z}^*)\rangle &= -\frac{i}{\hbar} H_{\text{sys}} |\psi(t, \mathbf{z}^*)\rangle + \sum_n L_n z_{t,n}^* |\psi(t, \mathbf{z}^*)\rangle \\ &\quad - \frac{1}{\hbar^2} \sum_n L_n^\dagger \int_0^t ds \alpha_n(t-s) \frac{\delta |\psi(t, \mathbf{z}^*)\rangle}{\delta z_{s,n}^*} \end{aligned} \quad (30)$$

in the small Hilbert space of the electronic degrees of freedom alone, with time-dependent complex numbers

$$z_{t,n}^* = -\frac{i}{\hbar} \sum_{\lambda} \kappa_{n\lambda} z_{n\lambda}^* e^{i\omega_{n\lambda} t} \quad (31)$$

and where

$$\begin{aligned} \alpha_n(t-s) &= \langle A_n(t) A_n^\dagger(s) \rangle_{T=0} = \langle 0 | A_n(t) A_n^\dagger(s) | 0 \rangle \\ &= \sum_{\lambda} |\kappa_{n\lambda}|^2 e^{-i\omega_{n\lambda}(t-s)} \end{aligned} \quad (32)$$

is the zero temperature bath correlation function of monomer n , which encodes the interaction of an electronic excitation with the environment of vibrations.

Note that in this case of zero temperature, $\alpha_n(t-s)$ is just the Fourier transform of the spectral density Eq. (13), i.e. $\alpha_n(\tau) = \int d\omega e^{-i\omega\tau} J_n(\omega)$.

For a non-Markovian bath, the solution of Eq. (30) is complicated due to the appearance of the memory integral over $\alpha_n(t-s)$ and the appearance of a functional derivative as an integrand. To deal with the functional derivative we follow Ref. [40] and write

$$\frac{\delta}{\delta z_{s,n}^*} |\psi(t, \mathbf{z}^*)\rangle = O^{(n)}(t, s, \mathbf{z}^*) |\psi(t, \mathbf{z}^*)\rangle \quad (33)$$

with an operator $O^{(n)}$ acting in the space of the electronic system part H_{sys} only. The operators $O^{(n)}(t, s, \mathbf{z}^*)$ have to obey the consistency condition

$$\partial_t \left(O^{(n)}(t, s, \mathbf{z}^*) |\psi(t, \mathbf{z}^*)\rangle \right) = \frac{\delta}{\delta z_{s,n}^*} \partial_t |\psi(t, \mathbf{z}^*)\rangle, \quad (34)$$

which leads, using Eq. (30) and introducing the abbreviation

$$\bar{O}^{(n)}(t, \mathbf{z}^*) = \frac{1}{\hbar^2} \int_0^t ds \alpha_n(t-s) O^{(n)}(t, s, \mathbf{z}^*), \quad (35)$$

to an evolution equation [53]

$$\begin{aligned} \partial_t O^{(m)}(t, s, \mathbf{z}^*) &= \left[-\frac{i}{\hbar} H_{\text{sys}}, O^{(m)}(t, s, \mathbf{z}^*) \right] \\ &+ \sum_n \left[L_n z_{t,n}^* - L_n^\dagger \bar{O}^{(n)}(t, \mathbf{z}^*), O^{(m)}(t, s, \mathbf{z}^*) \right] \\ &- \sum_n L_n^\dagger \frac{\delta \bar{O}^{(n)}(t, \mathbf{z}^*)}{\delta z_{s,m}^*}. \end{aligned} \quad (36)$$

The latter has to be solved with initial condition

$$O^{(n)}(s, s, \mathbf{z}^*) = L_n. \quad (37)$$

Finally, using Eq. (33) and (35), the evolution equation (30) turns into the linear non-Markovian QSD equation

$$\begin{aligned} \partial_t |\psi(t, \mathbf{z}^*)\rangle &= -\frac{i}{\hbar} H_{\text{sys}} |\psi(t, \mathbf{z}^*)\rangle \\ &+ \sum_n \left(L_n z_{t,n}^* - L_n^\dagger \bar{O}^{(n)}(t, \mathbf{z}^*) \right) |\psi(t, \mathbf{z}^*)\rangle. \end{aligned} \quad (38)$$

Due to the functional derivative appearing in Eq. (36), the operator $\bar{O}^{(n)}(t, \mathbf{z}^*)$ Eq. (35) cannot be evaluated in the general case. However, it can be obtained in some special cases, e.g. in the Markovian case (see Appendix A 2) and the case of non-interacting monomers (see Appendix A 1).

B. Absorption in the NMQSD approach

Using the NMQSD approach, the correlation function $M(t)$ of Eq. (21) can be calculated as follows. Inserting

the expansion Eq. (29) into Eq. (21) yields

$$M(t) = \mu_{\text{tot}}^2 \int \frac{d^2 \mathbf{z}}{\pi} e^{-|\mathbf{z}|^2} \langle \psi_0 | \psi(t, \mathbf{z}^*) \rangle \langle 0 | \mathbf{z} \rangle, \quad (39)$$

where $|\psi_0\rangle$ is given by Eq. (24). Here we used that $\langle 0 | e^{-iH_{\text{env}} t/\hbar}$ – which appears through the transformation to the interaction representation – is equal to $\langle 0 |$. From equation (39) we get [52]

$$M(t) = \mu_{\text{tot}}^2 \langle \psi_0 | \psi(t, \mathbf{z}^* = 0) \rangle \quad (40)$$

where $|\psi(t, \mathbf{z}^* = 0)\rangle$ can be obtained using Eq. (38) with $\mathbf{z}^* = 0$, i.e.

$$\begin{aligned} \partial_t |\psi(t, \mathbf{z}^* = 0)\rangle &= \\ \left(-\frac{i}{\hbar} H_{\text{sys}} - \sum_n L_n^\dagger \bar{O}^{(n)}(t, \mathbf{z}^* = 0) \right) &|\psi(t, \mathbf{z}^* = 0)\rangle \end{aligned} \quad (41)$$

with the initial condition $|\psi(t=0, \mathbf{z}^* = 0)\rangle = |\psi_0\rangle$. Note that due to the appearance of the functional derivative in Eq. (36) the determination of $\bar{O}^{(n)}(t)$ is still a formidable task.

V. THE ZEROth ORDER FUNCTIONAL EXPANSION (ZOFE) APPROXIMATION

The main task in the NMQSD approach is to obtain the operator $\bar{O}^{(n)}(t, \mathbf{z}^*)$ (and $O^{(n)}(t, s, \mathbf{z}^*)$ respectively) being defined in Eq. (35) (and Eq. (33)). An evolution equation for $O^{(n)}(t, s, \mathbf{z}^*)$ is given by Eq. (36). Although for the calculation of the zero temperature absorption spectrum from Eq. (41) only the values of $O^{(n)}(t, s, \mathbf{z}^*)$ for $\mathbf{z}^* = 0$ are needed, Eq. (36) contains the \mathbf{z}^* dependence via the functional derivative in a non-local way. To simplify Eq. (36) we follow Ref. [39] expanding the operator $O^{(n)}(t, s, \mathbf{z}^*)$ w.r.t. $z_{t,n}^*$ in a functional way and keep only the zeroth order term of the functional expansion. In other words, we approximate

$$O^{(n)}(t, s, \mathbf{z}^*) \approx O_0^{(n)}(t, s) \quad (42)$$

to be independent of \mathbf{z}^* and refer to Eq. (42) as the zeroth order functional expansion (ZOFE) approximation. Then, from Eq. (36) one obtains an approximate evolution equation [39]

$$\begin{aligned} \partial_t O_0^{(n)}(t, s) &= \left[-\frac{i}{\hbar} H_{\text{sys}}, O_0^{(n)}(t, s) \right] \\ &- \sum_m \left[L_m^\dagger \bar{O}_0^{(m)}(t), O_0^{(n)}(t, s) \right] \end{aligned} \quad (43)$$

with initial condition $O_0^{(n)}(s, s) = L_n$ (where we obtain $\bar{O}_0^{(n)}(t)$ from $O_0^{(n)}(t, s)$ via Eq. (35)). Inserting the approximate operator $\bar{O}_0^{(n)}(t)$ into Eq. (41) gives

$$\begin{aligned} \partial_t |\psi(t, \mathbf{z}^* = 0)\rangle &= \\ \left(-\frac{i}{\hbar} H_{\text{sys}} - \sum_n L_n^\dagger \bar{O}_0^{(n)}(t) \right) &|\psi(t, \mathbf{z}^* = 0)\rangle \end{aligned} \quad (44)$$

whose numerical implementation is straightforward [67]. To obtain the absorption spectrum of the aggregate, we solve equation (44) for the initial condition $|\psi(0, \mathbf{z}^* = 0)\rangle = |\psi_0\rangle$ given by Eq. (24). Then, we calculate the spectrum via Eqs. (40) and (15).

VI. PSEUDOMODE METHOD

As we will show in subsequent sections, the NMQSD approach in combination with the ZOFE approximation presented in Section IV offers a highly efficient method to calculate absorption spectra of molecular aggregates. However, it relies on the rather abstract ZOFE approximation made in Eq. (42). To obtain information about the accuracy of the approximation, in the following we will compare with exact calculations. It is clear that in general, an exact determination of aggregate spectra is a formidable task, impossible for arbitrary spectral densities and an arbitrary number N of monomers. In this section we review a method [42–44] that allows a numerically exact calculation of spectra for small aggregates for both correlation functions of the form

$$\alpha_n(t-s) = \sum_j \Gamma_{nj} e^{-i\Omega_{nj}(t-s) - \gamma_{nj}|t-s|} \quad (45)$$

which corresponds to the spectral density

$$J_n(\omega) = \frac{1}{\pi} \sum_j \Gamma_{nj} \frac{\gamma_{nj}}{(\omega - \Omega_{nj})^2 + \gamma_{nj}^2} \quad (46)$$

being a sum of Lorentzians centered at Ω_{nj} with width γ_{nj} . For the numerical implementation of the method, the number of Lorentzians which can be taken into account is limited (see examples in section VII). As a special case, the limit $\gamma_{nj} \rightarrow 0$ is included, i.e. the case of undamped vibrational modes, which has been extensively studied in the literature [35, 47, 49, 50, 54–56]. From the point of view of open system dynamics, the memory time of the environment is clearly infinite in such a case.

We want to point out that the NMQSD-ZOFE approach is not restricted to the special form (45) for the bath correlation function. However, note also that in principle an arbitrary bath correlation function can be approximated by a sum of exponentials in the form of Eq. (45) as discussed in Refs. [42, 43, 57].

A. The pseudomode (PM) Hamiltonian

In the pseudomode approach (see e.g. [42–44]) the system part of the aggregate Hamiltonian is enlarged. Apart from the electronic degrees of freedom, auxiliary vibrational degrees of freedom (pseudomodes) are included in the “system”, each coupled to a Markovian bath in a way specified below.

The Hamiltonian of the aggregate is written as

$$\tilde{H} = \tilde{H}^g |g_{el}\rangle\langle g_{el}| + \tilde{H}^e \sum_{n=1}^N |\pi_n\rangle\langle \pi_n| \quad (47)$$

where \tilde{H}^g is the vibrational Hamiltonian in the electronic ground state. The relevant Hamiltonian \tilde{H}^e of the aggregate in the excited electronic state is given by

$$\tilde{H}^e = \tilde{H}_{\text{sys}} + \tilde{H}_{\text{int}} + \tilde{H}_{\text{env}} \quad (48)$$

with the following choice of system, interaction and environment: the system part is chosen to be

$$\begin{aligned} \tilde{H}_{\text{sys}} = & H_{\text{sys}} + \sum_{n=1}^N \sum_j \hbar \Omega_{nj} b_{nj}^\dagger b_{nj} \\ & + \sum_{n=1}^N \sum_j \sqrt{\Gamma_{nj}} \left(L_n b_{nj}^\dagger + L_n^\dagger b_{nj} \right). \end{aligned} \quad (49)$$

Here, as before, the Hamiltonian H_{sys} is that of the purely electronic system given by Eq. (10). Additionally, for each monomer we include a set of vibrational modes (second term of Eq. (49)), where mode j of monomer n has a frequency Ω_{nj} (see Eq. (45)) and annihilation operator b_{nj} . These modes, enumerated with index j , are referred to as pseudomodes (PM). The third term of Eq. (49) describes the coupling of electronic excitation on monomer n to its PM j with coupling strength Γ_{nj} (see Eq. (45)). Each of the PMs has its own environment whose modes are enumerated with index ρ , so that in obvious notation,

$$\tilde{H}_{\text{env}} = \sum_{n=1}^N \sum_j \sum_\rho \hbar \tilde{\omega}_{nj\rho} \tilde{a}_{nj\rho}^\dagger \tilde{a}_{nj\rho}. \quad (50)$$

The PMs interact with their environments through

$$\tilde{H}_{\text{int}} = \sum_{n=1}^N \sum_j \sum_\rho \left(\tilde{\kappa}_{nj\rho}^* \tilde{a}_{nj\rho} b_{nj}^\dagger + \tilde{\kappa}_{nj\rho} \tilde{a}_{nj\rho}^\dagger b_{nj} \right), \quad (51)$$

where $\tilde{\kappa}_{nj\rho}$ denotes the coupling strength between PM j of monomer n to mode ρ of its local environment.

We now take the bath correlation functions of the PMs to read

$$\tilde{\alpha}_{nj}(t-s) = \sum_\rho |\tilde{\kappa}_{nj\rho}|^2 e^{-i\tilde{\omega}_{nj\rho}(t-s)} \equiv 2\hbar^2 \gamma_{nj} \delta(t-s), \quad (52)$$

i.e. the PMs couple to a Markovian environment (the parameter γ_{nj} is that of Eq. (45)). For a Markovian environment, however, we are in the regime of the standard Markov QSD of Section IV and find an exact solution (i.e. without applying the ZOFE approximation) for the time-dependent aggregate state and the absorption spectrum. Clearly, the price to pay is the need to propagate in the much larger Hilbert space of electronic and PM degrees of freedom.

We show in Appendix C that for a bath correlation function of the type of Eq. (45), the exact NMQSD approach without ZOFE approximation of Section IV and the PM method result in the same absorption spectra.

B. Absorption spectrum within the PM approach

As in Eq. (15) the absorption spectrum is calculated from

$$A(\nu) = \text{Re} \int_0^\infty dt e^{i\nu t} \tilde{M}(t), \quad (53)$$

where now instead of Eq. (40) we have

$$\tilde{M}(t) = \mu_{\text{tot}}^2 \langle \tilde{\psi}_0 | \tilde{\psi}(t) \rangle \quad (54)$$

with

$$|\tilde{\psi}_0\rangle = |\psi_0\rangle |g_{\text{PM}}\rangle. \quad (55)$$

Here, the initial electronic state $|\psi_0\rangle$ contains the action of the dipole operator, see Eq. (24) and $|g_{\text{PM}}\rangle$ is a product of the ground states of all PMs. As shown in detail in Appendix B, the state $|\tilde{\psi}(t)\rangle$ in Eq. (54) is obtained by solving the Schrödinger equation

$$\partial_t |\tilde{\psi}(t)\rangle = \left(-\frac{i}{\hbar} \tilde{H}_{\text{sys}} - \sum_{n=1}^N \sum_j \gamma_{nj} b_{nj}^\dagger b_{nj} \right) |\tilde{\psi}(t)\rangle \quad (56)$$

with the initial state $|\tilde{\psi}_0\rangle$ and \tilde{H}_{sys} from Eq. (49). We describe in Appendix B how this differential equation is solved numerically. There, we see that its solution becomes quite involved for large aggregates due to the explicit inclusion of the PMs into the “system”.

We note that Eq. (56) is just the Markov QSD equation with zero noise, and for the PM method takes the role of Eq. (41) in the NMQSD approach.

VII. COMPARISON BETWEEN ZOFE AND EXACT PM SPECTRA

In this section, we will compare absorption spectra calculated using the ZOFE approximation with numerically exact calculations obtained in the PM approach for spectral densities of the form Eq. (46). While being exact in the PM approach, the price one has to pay here is the increase of the number of degrees of freedom of the system part due to the inclusion of the PM into the system. This entails a rapid growth of the Hamiltonian matrix as the number M of PMs or the number N of monomers of the aggregate is increased. Thus, using the PM approach computer capabilities limit us to absorption spectra of aggregates with roughly $N = 2$ and $M \approx 6$ or $N = 3$ and $M \approx 5$ etc. The values of N and M we can handle, depend also on the coupling strength Γ_{nj} of the PM to

the electronic excitation: the larger the coupling Γ_{nj} , the more basis states have to be taken into account.

In the following, we consider a linear arrangement of monomers with identical properties, i.e. $\Gamma_{nj} = \Gamma_j$, $\Omega_{nj} = \Omega_j$, $\gamma_{nj} = \gamma_j$ for the j th PM of all monomers. For simplicity, we take all transition dipole moments of the monomers to be equal and consider only nearest neighbour interaction between the monomers, which we denote by V . We follow Simpson and Peterson [58] and speak of strong/intermediate/weak interaction, if V is larger/similar/smaller than the width of the monomer spectrum. As a parameter for the strength of the coupling of electronic excitation to the PMs we use the dimensionless Huang-Rhys factor [59]

$$X_j = \Gamma_j / (\hbar\Omega_j)^2. \quad (57)$$

This Huang-Rhys factor together with the ratios of the energies $\hbar\Omega_j$, $\hbar\gamma_j$ and V determines the shape of the absorption spectra.

First, we consider a spectral density that is a single Lorentzian centered at a frequency Ω . Here and in the following, we choose $\hbar\Omega$ as the unit of energy. Consequently, we express γ_j and Ω_j in units of Ω and V is given in units of $\hbar\Omega$. As a criterion for the agreement between a ZOFE spectrum and the corresponding PM spectrum we use the overlap of the areas of the two spectra. An overlap of 100% then means, that the two spectra are in perfect agreement. In Figure 1a this overlap is plotted against the monomer-monomer interaction V for the case of a dimer ($N = 2$) for a single Lorentzian spectral density with Huang-Rhys factor $X = 0.64$ and width $\gamma = 0.25$. From this plot we see, that the overlap has minima at roughly $V = \pm 0.4$. It increases rapidly going from there to smaller $|V|$ and increases (more slowly) going to larger $|V|$. At $V = 0$, the case of independent monomers, the overlap reaches 100%, since in this case the ZOFE is no approximation, but gives the exact result (see Appendix A 1). This can also be seen in Figure 1b, where the ZOFE (dashed line) and PM (solid line) monomer spectrum ($V = 0$) are shown for the considered spectral density $J(\omega)$ displayed in the inset of the figure. There, the dashed and the solid line are indistinguishable, since they lie exactly on top of each other, showing the perfect agreement between ZOFE and PM monomer spectrum. The monomer spectrum consists of broadened peaks separated by the vibrational energy $\hbar\Omega$ of the PM. We have chosen the zero of the energy axis to be located at the mean of the monomer spectrum. The values of the overlap in Figure 1a converge to 100% also for large $|V|$, showing that in the case of strong monomer-monomer interaction the ZOFE approximation becomes accurate too. In Figure 1a the values of V , for which the overlap is minimal, are indicated by two dashed vertical lines. Further vertical lines mark the four values of V , where the overlap reaches 97%. The corresponding dimer ZOFE (dashed line) and PM (solid line) spectra for the marked values of V are shown in Figure 1c-h. Figure 1c shows the ZOFE and PM spectrum for $V = -1.5$, having an over-

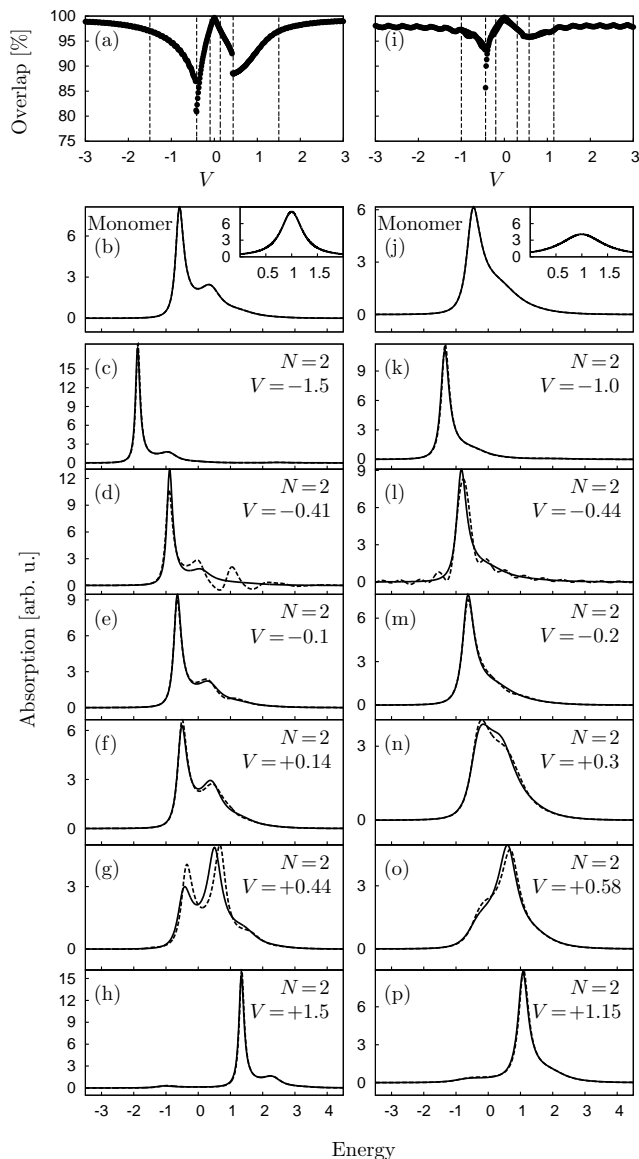


FIG. 1: Left column: (a) Overlap of ZOFE spectrum with PM spectrum over V for a dimer for a single Lorentzian spectral density centered at Ω with $X = 0.64$ and width $\gamma = 0.25\Omega$. (b) Monomer spectrum and spectral density $J(\omega)$ in units of $0.1\hbar^2\Omega$ (inset). (c)-(h) Corresponding dimer ZOFE spectra (dashed) and PM spectra (solid) for the values of V indicated by the dashed vertical lines in (a). Right column: same as left column, but with $\gamma = 0.5\Omega$.

lap of 97% corresponding to the left most vertical line in Figure 1a. As we can see here, this overlap value of 97% represents nearly perfect agreement between the spectra. The spectrum is much narrower than the monomer spectrum (note the different scales of the absorption axes). This narrowing in the case of strong interaction V (usually termed exchange narrowing) has also appeared in the investigation of Gaussian disorder [50, 60, 61], single vibrational modes [50] and in semi-empirical theories [31, 34]. Apparently, as for the monomer, in this case of

strong negative V the ZOFE approximation is quite accurate. Upon increasing V , one enters the intermediate interaction regime where discrepancies between ZOFE and PM spectra appear. At $V = -0.41$, where the overlap has a pronounced dip (see vertical line in Figure 1a), the agreement between the spectra is worst, shown in Figure 1d. However, when V is slightly changed from this value the agreement increases rapidly. Upon increasing V , at $V = -0.1$ the overlap reaches again 97% (see Figure 1e) owing to the fact, that in the region of weak inter-monomer interaction, where the spectra are similar to the monomer spectrum, the ZOFE approximation gives again accurate results. This also holds true for the case of positive weak interaction, as is demonstrated in Figure 1f and as can be seen from the overlap values in Figure 1a. Increasing V further to positive intermediate V again leads to discrepancies between the spectra as in the case of negative intermediate V . However, for positive V the largest deviation between ZOFE and PM spectrum at $V = +0.44$ (see Figure 1g), where the overlap is 88%, is not as large as the deviation at the overlap minimum for negative V . For strong positive interaction, there is again perfect agreement between ZOFE and PM spectra, as is shown in Fig. 1h for $V = +1.5$. These spectra have a strong blue shift w.r.t. the monomer spectrum and have become narrower again.

For a larger γ , which leads to a faster decay of the bath correlation function $\alpha(\tau)$ (see Eq. (45)), we expect that the agreement between ZOFE and PM spectra becomes better, since for infinitely fast decay (the Markov limit) ZOFE is exact (see Appendix A 2). That this reasoning is indeed correct is demonstrated in the right column of Fig. 1, where $\gamma = 0.5$, i.e. twice as large as in the left column. In the right column, the minimum values of the overlap of ZOFE and PM spectra are not as small as in the left column and the deviations between the spectra overall have become smaller compared to the left column.

Next, we consider the dependence of the agreement between the spectra on the Huang-Rhys factor X (and thus on the coupling strength Γ). In Fig. 2, overlap values and spectra are shown for a X roughly twice as large as in Fig. 1; the values of all other parameters are the same. The stronger coupling of the PM to the electronic excitation can clearly be seen in the monomer spectra (Fig. 2b, j) by an increase of the intensity of the second peak (located roughly at energy 0). The overlap of ZOFE and PM spectra in Fig. 2a shows a similar behaviour as before, but now the minimum has a very singular character for $\gamma = 0.25$. The agreement between ZOFE and PM spectra at the overlap minimum (see Fig. 2d) becomes worse compared to the case of $X = 0.64$ in Fig. 1d. However, for $\gamma = 0.5$ the largest deviation of the $X = 1.2$ spectra is smaller than the largest deviation of the $X = 0.64$ spectra. Comparing the overlap plots for $X = 0.64$ and $X = 1.2$ (Fig. 1a, i and Fig. 2a, i), one sees that the agreement between ZOFE and PM spectra in the case of $X = 0.64$ increases faster when going from the overlap minima to larger $|V|$ than in the case

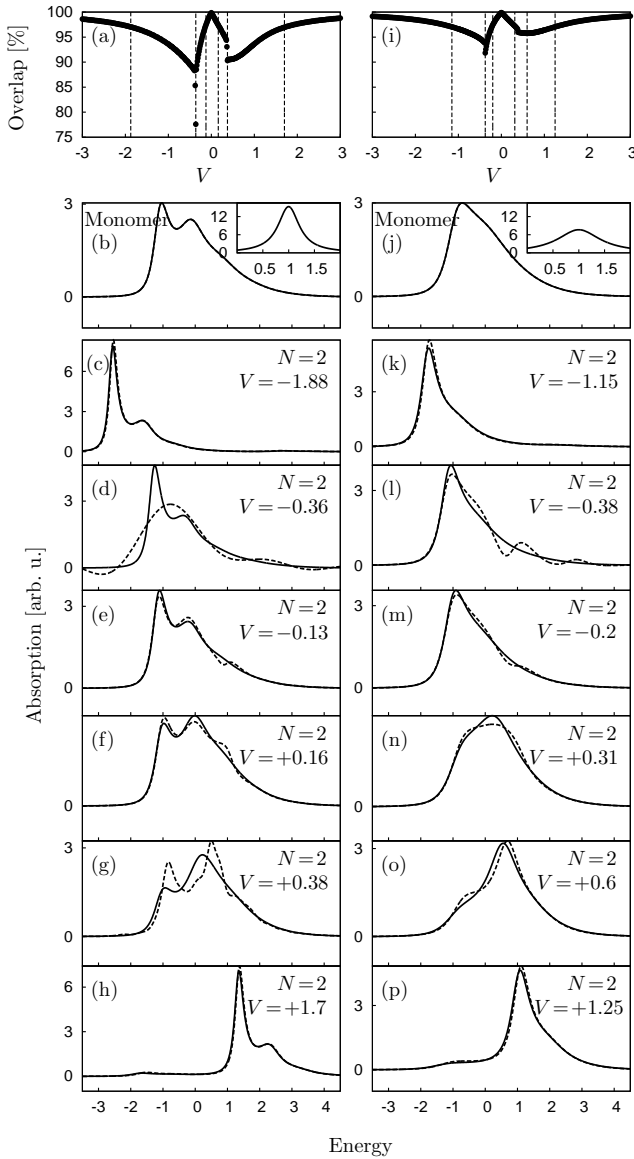


FIG. 2: Same as Fig. 1, but with $X = 1.2$.

of $X = 1.2$ (for both values of γ). This is also reflected in the larger values of $|V|$ to which one has to go in the case of $X = 1.2$ compared to $X = 0.64$ (for the respective γ), to achieve perfect agreement between the spectra (see Fig. 1c, h, k, p and Fig. 2c, h, k, p). These observations show that the quality of the ZOFE approximation depends on the magnitude of the inter-monomer interaction V relative to the magnitude of the coupling $\Gamma = (\hbar\Omega)^2 X$ of the electronic excitation to the PM.

In Figure 3, overlap values and absorption spectra for the same spectral densities as in Figure 1 are shown, but now for a trimer ($N = 3$). Here, the plots of the overlap against V show a greater number of local extrema. The trimer spectrum for the strong negative coupling $V = -1.5$ looks similar to the respective dimer spectrum, but is slightly narrower and has an additional small peak located roughly at an energy of $+2.1$, due to a second

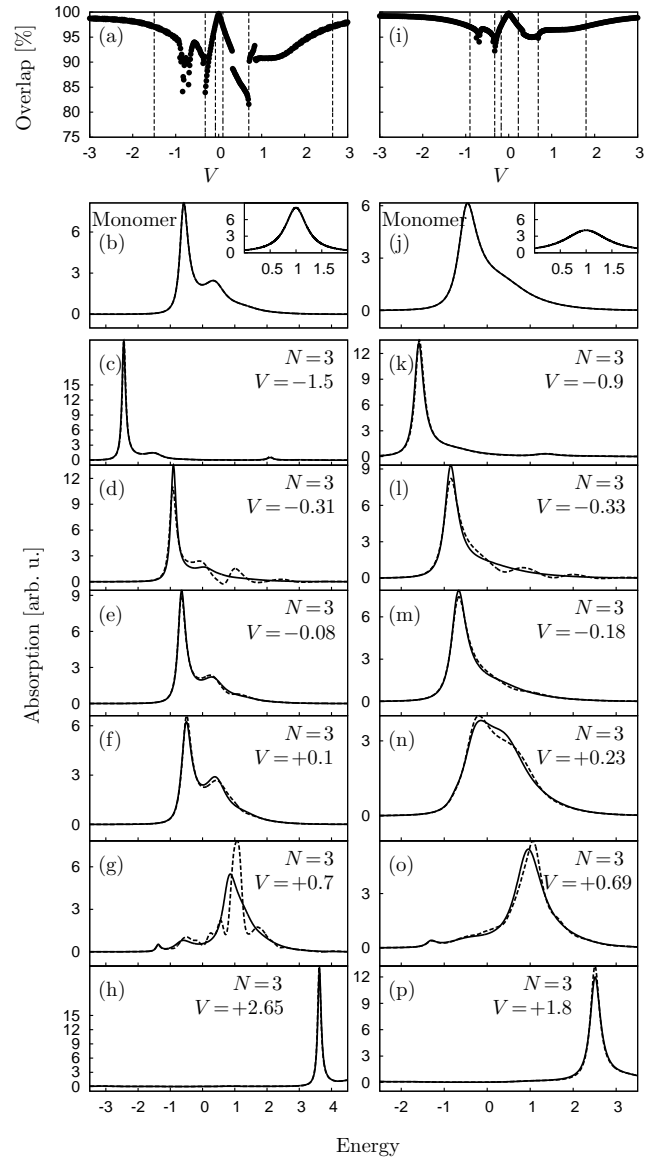


FIG. 3: Same as Fig. 1, but for the case of a trimer ($N = 3$).

allowed electronic transition. In this case, ZOFE and PM spectrum agree perfectly. Upon increasing V , as for the dimer we can identify the cases of strong and weak negative and positive interaction V , where there is good agreement between the spectra and the cases of negative and positive intermediate V , where the ZOFE and PM spectra show deviations. However, for the trimer we observe, that in the region of strong positive V to achieve perfect agreement between the spectra, we have to go to larger V , namely $V \approx +2.7$, compared to $V \approx +1.5$ for the dimer. Broadening of the spectral density by a factor of two (see right column) leads for the trimer spectra basically to the same effects and to the better agreement between solid and dashed spectra as for the dimer.

Our findings from the comparison of ZOFE spectra with exact PM spectra for the case of a spectral density with a single Lorentzian can be summarized as follows:

- 1) We always observe perfect agreement between ZOFE and PM spectra for strong and weak negative and positive inter-monomer interaction V .
- 2) There are deviations between the spectra in the intermediate V region (and clear resonance-like local minima in the overlap plots), that become smaller upon increasing the width γ of the spectral density.
- 3) Increasing the coupling Γ of the electronic excitation to the PM leads to a slower ascent of the agreement between the spectra when going from intermediate $|V|$ to larger $|V|$.
- 4) For the trimer, we find more local minima in the plots of the overlap against V than for the dimer.
- 5) To achieve perfect agreement between the spectra in the region of strong positive interaction V , in the case of the trimer V has to be larger than in the case of the dimer.

We have also performed exact calculations for more complex spectral densities, that are the sum of several Lorentzians. Here, we have observed similar trends as described above for the case of the single Lorentzian spectral density. As an example, in Fig. 4 ZOFE and PM monomer and dimer spectra are shown for a spectral density, that is the sum of six Lorentzians centered at different frequencies Ω_j with different Huang-Rhys factors X_j and widths γ_j . The six frequencies, where the Lorentzians are centered, range from $\Omega_1 = 0.23$ to $\Omega_6 = 1.61$ and the corresponding Huang-Rhys factors have different values $X_j = 0.4 \dots 0.24$. In the left column of Fig. 4, each Lorentzian has a width $\gamma_j = 0.25 \Omega_j$ and in the right column this width is increased by a factor two, i.e. $\gamma_j = 0.5 \Omega_j$. The calculation of a ZOFE dimer or trimer spectrum for the single Lorentzian spectral densities of the Figures 1-3, as well as for the spectral densities of Fig. 4 consisting of six Lorentzians, can be done within a few seconds on a standard PC. However, while the calculation of a PM dimer or trimer spectrum for the single Lorentzian spectral densities considered above also takes only a few seconds, the calculation of a PM dimer spectrum for the spectral densities consisting of six Lorentzians considered here took about six hours. This increase of the computational effort makes investigations involving hundreds of spectra like the evaluation of the overlap against V in Figures 1-3 very time-consuming. Therefore, in Fig. 4 we simply choose values for the interaction V , that in the case of a single Lorentzian spectral density considered before are typical for the V regions of perfect agreement and deviations between ZOFE and PM spectra. We see from Fig. 4, that as for the single Lorentzian spectral densities also in this case of a more complex spectral density we obtain perfect agreement between ZOFE and PM spectra for strong and weak negative and positive interaction V and deviations in the intermediate negative and positive V regions. And also here, the deviations become smaller when we go from the left column of Fig. 4 to the right column, i.e. increase the width of the Lorentzians of the spectral density from $\gamma_j = 0.25 \Omega_j$ to $\gamma_j = 0.5 \Omega_j$.

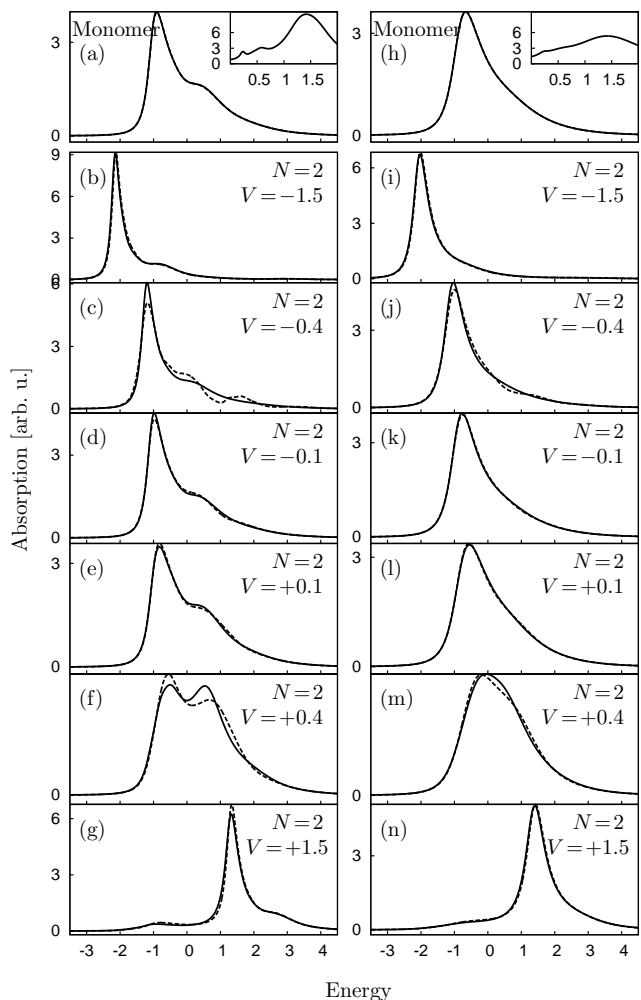


FIG. 4: Left column: (a) monomer spectrum for spectral density (shown in inset) that is a sum of six Lorentzians centered at different frequencies $\Omega_j = 0.23, 0.42, 0.57, 1.29, 1.41, 1.61$ with different Huang-Rhys factors $X_j = 0.4, 0.07, 0.18, 0.24, 0.12, 0.24$, where the width of each Lorentzian is $\gamma_j = 0.25 \Omega_j$. (b)-(g) Corresponding dimer ZOFE spectra (dashed) and PM spectra (solid) for different monomer-monomer interaction V . Right column: same as left column, but with $\gamma_j = 0.5 \Omega_j$ for each Lorentzian of the spectral density.

VIII. SUMMARY AND CONCLUSIONS

In this work we presented two different methods to calculate zero temperature absorption spectra of molecular aggregates, suited for situations in which the electronic excitation of a monomer couples to a structured phonon environment. Both methods are based on an open system approach, where the full Hamiltonian is divided into a “system” part, an “environment” and the interaction between them.

In the first method, we use the non-Markovian quantum state diffusion (NMQSD) approach, where the system contains only electronic degrees of freedom. To

tackle functional derivatives that appear in the NMQSD evolution equation the zeroth order functional expansion (ZOFE) approximation has been utilized. Although the NMQSD is based on a stochastic Schrödinger equation, we have shown that in the calculation of the zero temperature absorption spectrum the stochastic processes do not enter explicitly, so that only a deterministic equation has to be solved. Since in this method the system part contains only electronic degrees of freedom, i.e. the dimension of the considered single-exciton Hamiltonian is N for an N -mer, this approach can be applied to quite large systems with complex structured environments. The absorption spectrum of a 15-mer with a highly complex spectral density of the environmental modes for instance can be calculated within several minutes on a standard PC.

To calculate the absorption spectrum exactly and find out the accuracy of the ZOFE approximation used by the first method, we applied a second method, the method of pseudomodes (PM) described in section VI. Here, vibrational modes (pseudomodes) are included into the system part, which couple to the electronic excitation. The electronic excitation now is not coupled directly to an environment anymore, but each PM couples to its own Markovian bath of vibrational modes. This allows for a description of the problem via a Markovian quantum state diffusion (QSD) evolution equation, that can be solved numerically exact. For the practically important case of a spectral density of the environmental modes that is a sum of Lorentzians [42, 43, 57, 62] the absorption spectrum of the first method without applying the ZOFE approximation is equal to the absorption spectrum provided by the PM method (as we show in Appendix C). However, in the PM method the price one has to pay is that for each Lorentzian in the spectral density one PM is included into the system part, leading to a rapid growth of the dimension of the system Hamiltonian as the number N of monomers or the number of Lorentzians in the spectral density is increased. Thus, using the PM method we are at most able to calculate absorption spectra for a dimer with a spectral density of about six Lorentzians or a trimer with about five Lorentzians etc. due to limited computer capabilities. Here, the use of the Markovian QSD is advantageous over a propagation of a density matrix, having a size that is the square of the dimension of the used basis. In the QSD, for the calculation of the zero temperature absorption spectrum, only a system of differential equations with the size of the basis has to be solved. The spectrum is then found by a simple Fourier transformation. For our choice of the basis, the Hamiltonian becomes very sparse, allowing an efficient numerical propagation.

To investigate the applicability of the first method, that uses the ZOFE approximation, in section VII we compared the calculated spectra with spectra calculated using the PM method for small aggregates consisting of $N = 2$ or $N = 3$ monomers for spectral densities consisting of one and six Lorentzians. We always found perfect

agreement between ZOFE and PM spectra in the cases of strong or weak inter-monomer interaction (that is, when the interaction energy is large or small compared to the width of the monomer spectrum). However, we observed deviations between the spectra in the intermediate interaction regime, but these deviations become small upon increasing the width of the spectral density. In particular, for some narrow regions of the interaction energy, where we found a resonance-like decrease of the agreement between the spectra, the deviations became relevant. But also for these values of the interaction energy, the agreement becomes good again when the width of the spectral density is increased. When going from intermediate to strong inter-monomer interaction V , the agreement between the spectra increases. We found that in order to obtain the same degree of agreement for a stronger coupling Γ of the electronic excitation to the vibrations, V has to be chosen larger. For more complex spectral densities consisting of several Lorentzians we basically observed the same trends as for a single Lorentzian. Let us finally stress that over the entire range of the inter-monomer interaction V , the NMQSD-ZOFE approach leads to spectra with an overlap of more than 80–90% with the exact spectra, as can be seen in Figs. 1–3.

The NMQSD approach with the ZOFE approximation seems to be well suited to bridge the gap between the dimer case, which can be treated numerically exact for a large range of spectral densities (e.g. via the PM approach) and very large aggregates where semi-empirical approximations (like the coherent exciton scattering (CES) approximation [31, 34, 63]) lead to excellent agreement between theory and experiment.

As shown in Ref. [37], the NMQSD-ZOFE approach is not restricted to the calculation of absorption spectra, but allows also the calculation of fully time dependent quantities like the probability to find excitation on a certain monomer. Then however, in contrast to the present situation, stochastic processes will explicitly enter into the calculations.

Appendix A: Exactly solvable cases

1. Non-interacting monomers

Here we demonstrate that ZOFE leads to the exact spectrum for non-interacting monomers. To this end we show that the approximate zeroth order operator $O_0^{(n)}(t, s)$, which appears within ZOFE (see Eq. (42)), satisfies the fundamental consistency condition Eq. (34) or equivalently the evolution equation Eq. (36):

We insert $O_0^{(n)}(t, s)$ into Eq. (36). For non-interacting monomers, i.e. for $V_{nm} = 0$, we find

$$\partial_t O_0^{(n)}(t, s) = 0, \quad (\text{A1})$$

since the commutators vanish and the functional deriva-

tive yields zero. Equation (A1) together with the initial condition $O_0^{(n)}(s, s) = L_n$ (Eq. (37)) yields the constant

$$O_0^{(n)}(t, s) = L_n \quad (\text{A2})$$

without any approximation. Thus, ZOFE is exact for non-interacting monomers.

2. Markovian environment

Within the QSD approach of section IV we choose the bath correlation function $\alpha_n(t-s)$ to be delta-like, i.e.

$$\alpha_n(t-s) \equiv 2\hbar^2\theta_n\delta(t-s) \quad (\text{A3})$$

which amounts to a Markovian environment. Inserting Eqs. (A3) and (37) into Eq. (35) yields

$$\bar{O}^{(n)}(t, \mathbf{z}^*) = \theta_n L_n. \quad (\text{A4})$$

We see that in this Markov limit, the exact operator $\bar{O}^{(n)}(t, \mathbf{z}^*)$ is independent of \mathbf{z}^* and constant w.r.t. t . Thus, we find that ZOFE also contains the Markov limit. We insert Eq. (A4) into Eq. (38) and obtain the evolution equation

$$\begin{aligned} \partial_t |\psi(t, \mathbf{z}^*)\rangle &= -\frac{i}{\hbar} H_{\text{sys}} |\psi(t, \mathbf{z}^*)\rangle \\ &+ \sum_n (L_n z_{t,n}^* - \theta_n L_n^\dagger L_n) |\psi(t, \mathbf{z}^*)\rangle. \end{aligned} \quad (\text{A5})$$

which is the well-known linear Markov QSD equation [64].

Appendix B: Absorption in the pseudomode approach

In this section, we show how we obtain the absorption spectrum using the approach of pseudomodes of Section VI. As the initial state of the aggregate we take

$$|\tilde{\Phi}(t=0)\rangle = |g_{\text{el}}\rangle |g_{\text{PM}}\rangle |\tilde{0}\rangle, \quad (\text{B1})$$

where $|g_{\text{el}}\rangle$ is the product of all monomer electronic ground states given by Eq. (4). The state $|g_{\text{PM}}\rangle$ denotes the product of the ground states of all PMs and $|\tilde{0}\rangle$ is the bath state in which all bath modes are in their ground states. Analogously to Section III, the cross section for absorption of light can be obtained from Eq. (53) with the dipole correlation function

$$\tilde{M}(t) = \langle \tilde{\Phi}(t=0) | \hat{\mu} \cdot \mathcal{E} e^{-i\tilde{H}t/\hbar} \hat{\mu} \cdot \mathcal{E}^* | \tilde{\Phi}(t=0) \rangle, \quad (\text{B2})$$

where $\hat{\mu}$ is the total dipole operator of the aggregate, given by Eq. (17). As in Section III by using Eqs. (17) and (19), we obtain

$$\tilde{M}(t) = \mu_{\text{tot}}^2 \langle \tilde{\Psi}(t=0) | \tilde{\Psi}(t) \rangle \quad (\text{B3})$$

with the normalized aggregate states

$$|\tilde{\Psi}(t=0)\rangle = |\tilde{\psi}_0\rangle |\tilde{0}\rangle \quad (\text{B4})$$

and with $|\tilde{\psi}_0\rangle$ given by Eq. (55) and

$$|\tilde{\Psi}(t)\rangle = \exp(-i\tilde{H}^e t/\hbar) |\tilde{\Psi}(t=0)\rangle. \quad (\text{B5})$$

The prefactor μ_{tot} in Eq. (B3) is defined in Eq. (20). Similarly as in Section IV B, we use the expansion

$$|\tilde{\Psi}(t)\rangle = \int \frac{d^2\tilde{\mathbf{z}}}{\pi} e^{-|\tilde{\mathbf{z}}|^2} |\tilde{\psi}(t, \tilde{\mathbf{z}}^*)\rangle |\tilde{\mathbf{z}}\rangle. \quad (\text{B6})$$

Here, $|\tilde{z}_{nj\rho}\rangle = \exp(\tilde{z}_{nj\rho} \tilde{a}_{nj\rho}^\dagger) |\tilde{0}_{nj\rho}\rangle$ denote Bargmann coherent bath states, and $|\tilde{\mathbf{z}}\rangle = \prod_n \prod_j \prod_\rho |\tilde{z}_{nj\rho}\rangle$. From Eqs. (B4), (B6), and (B3), we obtain

$$\tilde{M}(t) = \mu_{\text{tot}}^2 \langle \tilde{\psi}_0 | \tilde{\psi}(t, \tilde{\mathbf{z}}^* = 0) \rangle. \quad (\text{B7})$$

We may determine the state $|\tilde{\psi}(t, \tilde{\mathbf{z}}^* = 0)\rangle$ using the QSD approach analogously to Section IV, now for a memory-less (Markovian) environment (see also appendix A 2). First, \tilde{H}^e of Eq. (48) is transformed to the interaction representation w.r.t. \tilde{H}_{env} Eq. (50) to find

$$\tilde{H}^e(t) = \tilde{H}_{\text{sys}} + \sum_{n=1}^N \sum_j \left(\tilde{L}_{nj} \tilde{A}_{nj}^\dagger(t) + \tilde{L}_{nj}^\dagger \tilde{A}_{nj}(t) \right) \quad (\text{B8})$$

with

$$\tilde{A}_{nj}(t) \equiv \sum_\rho \tilde{\kappa}_{nj\rho}^* e^{-i\tilde{\omega}_{nj\rho} t} \tilde{a}_{nj\rho} \quad (\text{B9})$$

and where

$$\tilde{L}_{nj} \equiv b_{nj}. \quad (\text{B10})$$

From the definition of $\tilde{A}_{nj}(t)$ Eq. (B9), we get the bath correlation function

$$\begin{aligned} \tilde{\alpha}_{nj}(t-s) &\equiv \langle \tilde{0} | \tilde{A}_{nj}(t) \tilde{A}_{nj}^\dagger(s) | \tilde{0} \rangle \\ &= \sum_\rho |\tilde{\kappa}_{nj\rho}|^2 e^{-i\tilde{\omega}_{nj\rho}(t-s)}, \end{aligned} \quad (\text{B11})$$

where $|\tilde{0}\rangle$ denotes the state in which all bath modes are in their ground states.

We want to solve the Schrödinger equation

$$i\hbar\partial_t |\tilde{\Psi}(t)\rangle = \tilde{H}^e(t) |\tilde{\Psi}(t)\rangle. \quad (\text{B12})$$

Inserting the expansion Eq. (B6) into Eq. (B12) we obtain

$$\begin{aligned} \partial_t |\tilde{\psi}(t, \tilde{\mathbf{z}}^*)\rangle &= -\frac{i}{\hbar} \tilde{H}_{\text{sys}} |\tilde{\psi}(t, \tilde{\mathbf{z}}^*)\rangle + \sum_{n,j} \tilde{L}_{nj} \tilde{z}_{t,nj}^* |\tilde{\psi}(t, \tilde{\mathbf{z}}^*)\rangle \\ &- \frac{1}{\hbar^2} \sum_{n,j} \tilde{L}_{nj}^\dagger \int_0^t ds \tilde{\alpha}_{nj}(t-s) \frac{\delta |\tilde{\psi}(t, \tilde{\mathbf{z}}^*)\rangle}{\delta \tilde{z}_{s,nj}^*} \end{aligned} \quad (\text{B13})$$

with time-dependent complex numbers

$$\tilde{z}_{t,nj}^* = -\frac{i}{\hbar} \sum_{\rho} \tilde{\kappa}_{nj\rho} \tilde{z}_{nj\rho}^* e^{i\tilde{\omega}_{nj\rho}t}. \quad (\text{B14})$$

From Eq. (52) we have $\tilde{\alpha}_{nj}(t-s) \propto \delta(t-s)$, i.e. the environment of the pseudomodes is Markovian. Now, we make use of this fact by inserting Eq. (52) into Eq. (B13) and obtain

$$\begin{aligned} \partial_t |\tilde{\psi}(t, \tilde{\mathbf{z}}^*)\rangle &= -\frac{i}{\hbar} \tilde{H}_{\text{sys}} |\tilde{\psi}(t, \tilde{\mathbf{z}}^*)\rangle \\ &+ \sum_{n,j} \tilde{L}_{nj} \tilde{z}_{t,nj}^* |\tilde{\psi}(t, \tilde{\mathbf{z}}^*)\rangle \\ &- \sum_{n,j} \gamma_{nj} \tilde{L}_{nj}^{\dagger} \tilde{L}_{nj} |\tilde{\psi}(t, \tilde{\mathbf{z}}^*)\rangle. \end{aligned} \quad (\text{B15})$$

In the case $\tilde{\mathbf{z}}^* = 0$ equation (B15) yields the evolution equation (56) of Section VIB, i.e.

$$\begin{aligned} \partial_t |\tilde{\psi}(t, \tilde{\mathbf{z}}^* = 0)\rangle &= -\frac{i}{\hbar} \tilde{H}_{\text{sys}} |\tilde{\psi}(t, \tilde{\mathbf{z}}^* = 0)\rangle \\ &- \sum_{n,j} \gamma_{nj} \tilde{L}_{nj}^{\dagger} \tilde{L}_{nj} |\tilde{\psi}(t, \tilde{\mathbf{z}}^* = 0)\rangle. \end{aligned} \quad (\text{B16})$$

In order to obtain the absorption spectrum, this equation is solved for the initial state $|\tilde{\psi}_0\rangle$.

a. Numerical implementation

We express the Schrödinger equation Eq. (56) in a basis of product states

$$|\theta_n^{\beta}\rangle \equiv |\pi_n\rangle \prod_{n=1}^N \prod_j |\beta_{nj}\rangle \quad (\text{B17})$$

with vibrational eigenstates $|\beta_{nj}\rangle$ of PM j in the electronic ground state of monomer n , i.e. the states $|\beta_{nj}\rangle$ satisfy

$$\hbar\Omega_{nj} b_{nj}^{\dagger} b_{nj} |\beta_{nj}\rangle = \hbar\Omega_{nj} \beta_{nj} |\beta_{nj}\rangle. \quad (\text{B18})$$

From the Schrödinger equation Eq. (56) we obtain a system of coupled differential equations for the components $\langle \theta_n^{\beta} | \tilde{\psi}(t) \rangle$ w.r.t. the states Eq. (B17)

$$\begin{aligned} \partial_t \langle \theta_n^{\beta} | \tilde{\psi}(t) \rangle &= \\ &- \frac{i}{\hbar} \left(\varepsilon_n + \sum_{m=1}^N \sum_j (\hbar\Omega_{mj} - i\hbar\gamma_{mj}) \beta_{mj} \right) \langle \theta_n^{\beta} | \tilde{\psi}(t) \rangle \\ &+ \frac{i}{\hbar} \sum_j \sqrt{\Gamma_{nj}} \sqrt{\beta_{nj}} \langle \theta_n^{(\beta_{11}\dots\beta_{nj-1}\dots)} | \tilde{\psi}(t) \rangle \\ &+ \frac{i}{\hbar} \sum_j \sqrt{\Gamma_{nj}} \sqrt{\beta_{nj} + 1} \langle \theta_n^{(\beta_{11}\dots\beta_{nj}+1\dots)} | \tilde{\psi}(t) \rangle \\ &- \frac{i}{\hbar} \sum_{m \neq n}^N V_{nm} \langle \theta_m^{\beta} | \tilde{\psi}(t) \rangle. \end{aligned} \quad (\text{B19})$$

Since the corresponding matrix is very sparse, we are able to calculate the absorption spectrum taking into account a few PMs per monomer. For the calculation of the dipole correlation function Eq. (54), we choose the initial state Eq. (55) to be real-valued. On that condition and by using the fact that the Hamiltonian corresponding to the system of equations Eq. (B19) is symmetric (it is equal to its transpose), we can calculate the value of the dipole correlation function at time $2t$ through [65]

$$\tilde{M}(2t) = \mu_{\text{tot}}^2 \left(\langle \tilde{\psi}(t) | \right)^* | \tilde{\psi}(t) \rangle, \quad (\text{B20})$$

where the star $*$ denotes the complex conjugate. That is, the time we need to propagate the wavefunction numerically shortens by a factor of two. Note, that for complex initial wavefunctions the efficient calculation scheme Eq. (B20) is no longer applicable.

Appendix C: Equality of NMQSD spectrum and PM spectrum

In this section, we show that the absorption spectrum obtained from the NMQSD approach is equal to the spectrum obtained from the PM method for a bath correlation function consisting of a sum of exponentials as in Eq. (45). This equivalence holds true provided the parameters (Ω_{nj} , γ_{nj} , and Γ_{nj}) of the pseudomode description are taken from the corresponding bath correlation function of the NMQSD approach.

We start with the Hamiltonian of the PM approach defined by Eqs. (48)-(51). It can be written as

$$\tilde{H}^e = H_{\text{sys}} + \sum_{n=1}^N \sum_j \sqrt{\Gamma_{nj}} \left(L_n b_{nj}^{\dagger} + L_n^{\dagger} b_{nj} \right) + H_{\text{vib}}. \quad (\text{C1})$$

Here, H_{sys} is the Hamiltonian containing only electronic degrees of freedom and

$$\begin{aligned} H_{\text{vib}} &\equiv \sum_{n=1}^N \sum_j \hbar\Omega_{nj} b_{nj}^{\dagger} b_{nj} \\ &+ \sum_{n=1}^N \sum_j \sum_{\rho} \left(\tilde{\kappa}_{nj\rho}^* \tilde{a}_{nj\rho} b_{nj}^{\dagger} + \tilde{\kappa}_{nj\rho} \tilde{a}_{nj\rho}^{\dagger} b_{nj} \right) \\ &+ \sum_{n=1}^N \sum_j \sum_{\rho} \hbar\tilde{\omega}_{nj\rho} \tilde{a}_{nj\rho}^{\dagger} \tilde{a}_{nj\rho}, \end{aligned} \quad (\text{C2})$$

contains the pseudomodes, their Markovian environments, and their respective couplings. We diagonalize H_{vib} , i.e. we write

$$H_{\text{vib}} = \sum_{n=1}^N \sum_j \sum_{\sigma} \hbar\tilde{\omega}_{nj\sigma} c_{nj\sigma}^{\dagger} c_{nj\sigma}, \quad (\text{C3})$$

with new frequencies $\hat{\omega}_{nj\sigma}$ and new annihilation operators $c_{nj\sigma}$ that are a linear combination

$$c_{nj\sigma} = \chi_{nj\sigma}^* b_{nj} + \sum_{\rho} \zeta_{nj\rho\sigma} \tilde{a}_{nj\rho} \quad (\text{C4})$$

of the original ones and with

$$b_{nj} = \sum_{\sigma} \chi_{nj\sigma} c_{nj\sigma}, \quad (\text{C5})$$

where the $\chi_{nj\sigma}$ and $\zeta_{nj\rho\sigma}$ are complex coefficients (this is shown in Ref. [66] for real coefficients and can be extended easily to the present case). With Eqs. (C3) and (C5) \tilde{H}^e Eq. (C1) has the form of H^e Eqs. (9)-(12) and we can derive a Schrödinger equation in the reduced space of H_{sys} analogously to section IV. Transforming \tilde{H}^e from Eq. (C1) to the interaction representation w.r.t. H_{vib} yields

$$\tilde{H}^e(t) = H_{\text{sys}} + \sum_{n=1}^N (L_n B_n^\dagger(t) + L_n^\dagger B_n(t)), \quad (\text{C6})$$

with

$$B_n(t) \equiv \sum_j \sqrt{\Gamma_{nj}} b_{nj}(t) \quad (\text{C7})$$

and

$$b_{nj}(t) \equiv e^{iH_{\text{vib}}t/\hbar} b_{nj} e^{-iH_{\text{vib}}t/\hbar}. \quad (\text{C8})$$

Note that Eq. (C6) has the same structure as Eq. (25). Using Eqs. (C5) and (C3), from Eq. (C8) we obtain

$$b_{nj}(t) = \sum_{\sigma} \chi_{nj\sigma} c_{nj\sigma} e^{-i\hat{\omega}_{nj\sigma}t}. \quad (\text{C9})$$

From Eqs. (C9) and (C7), we get

$$B_n(t) = \sum_j \sqrt{\Gamma_{nj}} \sum_{\sigma} \chi_{nj\sigma} c_{nj\sigma} e^{-i\hat{\omega}_{nj\sigma}t}. \quad (\text{C10})$$

Next we insert the expansion

$$|\tilde{\Psi}(t)\rangle = \int \frac{d^2\hat{\mathbf{z}}}{\pi} e^{-|\hat{\mathbf{z}}|^2} |\varphi(t, \hat{\mathbf{z}}^*)\rangle |\hat{\mathbf{z}}\rangle \quad (\text{C11})$$

w.r.t. Bargmann coherent states $|\hat{\mathbf{z}}_{nj\sigma}\rangle = \exp(\hat{\mathbf{z}}_{nj\sigma} c_{nj\sigma}^\dagger) |\hat{\xi}_{nj\sigma}^0\rangle$, where $|\hat{\mathbf{z}}\rangle = \prod_n \prod_j \prod_{\sigma} |\hat{\mathbf{z}}_{nj\sigma}\rangle$, into the Schrödinger equation

$$i\hbar\partial_t |\tilde{\Psi}(t)\rangle = \tilde{H}^e(t) |\tilde{\Psi}(t)\rangle \quad (\text{C12})$$

for the total state $|\tilde{\Psi}(t)\rangle$. This leads to an evolution equation

$$\begin{aligned} \partial_t |\varphi(t, \hat{\mathbf{z}}^*)\rangle &= -\frac{i}{\hbar} H_{\text{sys}} |\varphi(t, \hat{\mathbf{z}}^*)\rangle + \sum_n L_n \hat{z}_{t,n}^* |\varphi(t, \hat{\mathbf{z}}^*)\rangle \\ &\quad - \frac{1}{\hbar^2} \sum_n L_n^\dagger \int_0^t ds \beta_n(t-s) \frac{\delta |\varphi(t, \hat{\mathbf{z}}^*)\rangle}{\delta \hat{z}_{s,n}^*} \end{aligned} \quad (\text{C13})$$

for the state $|\varphi(t, \hat{\mathbf{z}}^*)\rangle$ in the Hilbert space of the original “system” with Hamiltonian H_{sys} . In Eq. (C13), the time-dependent complex numbers

$$\hat{z}_{t,n}^* = -\frac{i}{\hbar} \sum_j \sqrt{\Gamma_{nj}} \sum_{\sigma} \chi_{nj\sigma}^* \hat{z}_{nj\sigma} e^{i\hat{\omega}_{nj\sigma}t} \quad (\text{C14})$$

and the correlation functions

$$\begin{aligned} \beta_n(t-s) &= \langle B_n(t) B_n^\dagger(s) \rangle_{T=0} = \langle \hat{0} | B_n(t) B_n^\dagger(s) | \hat{0} \rangle \\ &= \sum_j \Gamma_{nj} \sum_{\sigma} |\chi_{nj\sigma}|^2 e^{-i\hat{\omega}_{nj\sigma}(t-s)} \end{aligned} \quad (\text{C15})$$

are used.

The NMQSD absorption spectrum is equal to the PM spectrum if the corresponding time correlation functions $M(t)$ of the NMQSD approach and $\tilde{M}(t)$ of the PM approach are equal (see Eqs. (15) and (53)). From Eqs. (B3)-(B5) and Eq. (C11) we get

$$\tilde{M}(t) = \mu_{\text{tot}}^2 \langle \tilde{0} | \langle g_{\text{PM}} | \langle \psi_0 | \int \frac{d^2\hat{\mathbf{z}}}{\pi} e^{-|\hat{\mathbf{z}}|^2} |\varphi(t, \hat{\mathbf{z}}^*)\rangle |\hat{\mathbf{z}}\rangle, \quad (\text{C16})$$

similar to Eq. (39). Because of equation (C4), we have

$$|g_{\text{PM}}\rangle |\tilde{0}\rangle = |\hat{0}\rangle. \quad (\text{C17})$$

Using Eq. (C17), equation (C16) yields

$$\tilde{M}(t) = \mu_{\text{tot}}^2 \langle \psi_0 | \varphi(t, \hat{\mathbf{z}}^* = 0) \rangle \quad (\text{C18})$$

with the initial state

$$|\varphi(t=0, \hat{\mathbf{z}}^* = 0)\rangle = |\psi_0\rangle. \quad (\text{C19})$$

The time correlation function $\tilde{M}(t)$ Eq. (C18) of the PM method is equal to $M(t)$ Eq. (40) of the NMQSD approach, if the state $|\varphi(t, \hat{\mathbf{z}}^* = 0)\rangle$ is equal to $|\psi(t, \mathbf{z}^* = 0)\rangle$ for all times t . Thus, we next show that Eq. (C13) for $\hat{\mathbf{z}}^* = 0$ is equivalent to Eq. (30) for $\mathbf{z}^* = 0$. According to Eq. (33), we replace the functional derivative in Eq. (30) by the operator $O^{(n)}(t, s, \mathbf{z}^*)$ and the functional derivative in Eq. (C13) by an operator $\hat{O}^{(n)}(t, s, \hat{\mathbf{z}}^*)$. Note, however, that we do not make the ZOFE approximation, so that our treatment remains exact. Following Ref. [39], one can expand the operators $O^{(n)}(t, s, \mathbf{z}^*)$ and $\hat{O}^{(n)}(t, s, \hat{\mathbf{z}}^*)$ w.r.t. the functionals $z_{t,n}^*$ and $\hat{z}_{t,n}^*$ and obtain a hierarchy of differential equations for the different orders $O_0^{(n)}, O_1^{(n)}, \dots$ of the expansion. These differential equations do not contain $z_{t,n}^*$ (and $\hat{z}_{t,n}^*$ respectively) anymore and they are the same for $O^{(n)}(t, s, \mathbf{z}^*)$ and $\hat{O}^{(n)}(t, s, \hat{\mathbf{z}}^*)$. Thus we have $O_0^{(n)} = \hat{O}_0^{(n)}$, $O_1^{(n)} = \hat{O}_1^{(n)}$, \dots . Now it only remains to show that in Eqs. (30) and (C13) $\alpha_n(t-s) = \beta_n(t-s)$. This we will show in the following. We consider the time derivative of Eq. (C8)

$$\partial_t b_{nj}(t) = \frac{i}{\hbar} e^{iH_{\text{vib}}t/\hbar} [H_{\text{vib}}, b_{nj}] e^{-iH_{\text{vib}}t/\hbar}. \quad (\text{C20})$$

Inserting the definition of H_{vib} Eq. (C2) into Eq. (C20) yields

$$\partial_t b_{nj}(t) = -i\Omega_{nj} b_{nj}(t) - \frac{i}{\hbar} \sum_{\rho} \tilde{\kappa}_{nj\rho}^* \tilde{a}_{nj\rho}(t), \quad (\text{C21})$$

with

$$\tilde{a}_{nj\rho}(t) \equiv e^{iH_{\text{vib}}t/\hbar} \tilde{a}_{nj\rho} e^{-iH_{\text{vib}}t/\hbar}. \quad (\text{C22})$$

Taking the time derivative of Equation (C22) and inserting the definition of H_{vib} Eq. (C2) yields

$$\partial_t \tilde{a}_{nj\rho}(t) = -i\tilde{\omega}_{nj\rho} \tilde{a}_{nj\rho}(t) - \frac{i}{\hbar} \tilde{\kappa}_{nj\rho} b_{nj}(t). \quad (\text{C23})$$

We integrate Eq. (C23) and obtain

$$\begin{aligned} \tilde{a}_{nj\rho}(t) &= e^{-i\tilde{\omega}_{nj\rho}t} \tilde{a}_{nj\rho}(0) \\ &\quad - \frac{i}{\hbar} \tilde{\kappa}_{nj\rho} \int_0^t ds e^{-i\tilde{\omega}_{nj\rho}(t-s)} b_{nj}(s). \end{aligned} \quad (\text{C24})$$

Inserting $\tilde{a}_{nj\rho}(t)$ Eq. (C24) into Eq. (C21) yields

$$\begin{aligned} \partial_t b_{nj}(t) &= -i\Omega_{nj} b_{nj}(t) \\ &\quad - \frac{1}{\hbar^2} \int_0^t ds \sum_{\rho} |\tilde{\kappa}_{nj\rho}|^2 e^{-i\tilde{\omega}_{nj\rho}(t-s)} b_{nj}(s) \\ &\quad - \frac{i}{\hbar} \tilde{A}_{nj}(t) \end{aligned} \quad (\text{C25})$$

with $\tilde{A}_{nj}(t)$ given by Eq. (B9). The $\tilde{A}_{nj}(t)$ are correlated with the function $\tilde{\alpha}_{nj}(t-s)$ given by Eq. (B11).

Using the PM method the bath is Markovian, so that $\tilde{\alpha}_{nj}(t-s)$ is proportional to a delta function Eq. (52). Inserting Eq. (52) into Eq. (C25) leads to

$$\partial_t b_{nj}(t) = -i\Omega_{nj} b_{nj}(t) - \gamma_{nj} b_{nj}(t) - \frac{i}{\hbar} \tilde{A}_{nj}(t). \quad (\text{C26})$$

Integration of Eq. (C26) yields

$$\begin{aligned} b_{nj}(t) &= e^{-i\Omega_{nj}t - \gamma_{nj}t} b_{nj}(0) \\ &\quad - \frac{i}{\hbar} \int_0^t ds e^{-i\Omega_{nj}(t-s) - \gamma_{nj}(t-s)} \tilde{A}_{nj}(s). \end{aligned} \quad (\text{C27})$$

We now insert $b_{nj}(t)$ Eq. (C27) into the correlation function

$$\langle b_{nj}(t) b_{nj}^\dagger(s) \rangle_{T=0} = \langle \hat{0} | b_{nj}(t) b_{nj}^\dagger(s) | \hat{0} \rangle \quad (\text{C28})$$

and obtain (by separately considering the cases $t < s$ and $t > s$)

$$\langle b_{nj}(t) b_{nj}^\dagger(s) \rangle_{T=0} = e^{-i\Omega_{nj}(t-s) - \gamma_{nj}|t-s|}. \quad (\text{C29})$$

Finally, Eq. (C29) together with the definition of $B_n(t)$ from Eq. (C7) and Eq. (C15) yields the result

$$\beta_n(t-s) = \sum_j \Gamma_{nj} e^{-i\Omega_{nj}(t-s) - \gamma_{nj}|t-s|}, \quad (\text{C30})$$

which is equal to the special bath correlation function $\alpha_n(t-s)$ given by Eq. (45) for the NMQSD approach.

Thus, we have shown that the absorption spectrum we obtain from the PM method of section VI is equal to the spectrum we get by using the NMQSD approach according to section IV.

Acknowledgments

We thank John S. Briggs, Wolfgang Wolff, Alexander Croy, and Sebastian Wüster for many helpful discussions.

-
- [1] A. Davydov, *Theory of Molecular Excitons* (McGraw-Hill, 1962).
- [2] M. Schwoerer and H. Wolf, *Organic Molecular Solids* (Wiley-VCH, 2006).
- [3] G. Scheibe, *Angewandte Chemie* **49**, 563 (1936).
- [4] E. E. Jelley, *Nature* **138**, 1009 (1936).
- [5] G. Scheibe, *Kolloid-Zeitschrift* **82**, 1 (1938).
- [6] J. Franck and E. Teller, *J. Chem. Phys.* **6**, 861 (1938).
- [7] T. Kobayashi, ed., *J-Aggregates* (World Scientific, 1996).
- [8] H. van Amerongen, L. Valkunas, and R. van Grondelle, *Photosynthetic Excitons* (World Scientific, Singapore, 2000).
- [9] T. Renger, V. May, and O. Kühn, *Physics Reports* **343**, 137 (2001).
- [10] R. van Grondelle and V. I. Novoderezhkin, *Phys. Chem. Chem. Phys.* **8**, 793 (2006).
- [11] A. Freiberg, M. Rätsep, K. Timpmann, and G. Trinkunas, *Chem. Phys.* **357**, 102 (2009), excited State Dynamics in Light Harvesting Materials.
- [12] F. Robicheaux, J. V. Hernández, T. Topçu, and L. D. Noordam, *Physical Review A* **70**, 042703 (2004).
- [13] W. R. Anderson, J. R. Veale, and T. F. Gallagher, *Physical Review Letters* **80**, 249 (1998).
- [14] O. Mülken, A. Blumen, T. Amthor, C. Giese, M. Reetz-Lamour, and M. Weidemüller, *Phys. Rev. Lett.* **99**, 090601 (2007).
- [15] C. Ates, A. Eisfeld, and J. M. Rost, *New Journal of Physics* **10**, 045030 (2008).
- [16] S. Wüster, C. Ates, A. Eisfeld, and J. M. Rost, *Phys. Rev. Lett.* **105**, 053004 (2010).
- [17] H. Matsueda, K. Leosson, Z. C. Xu, J. M. Hvam, Y. D. A. Hartmann, and E. Kapon, *IEEE Trans. Nanotechnol.* **3**, 318 (2004).
- [18] B. W. Lovett, J. H. Reina, A. Nazir, B. Kothari, and

- G. A. D. Briggs, Phys. Lett. A **315**, 136 (2003).
- [19] W. Rechberger, A. Hohenau, A. Leitner, J. R. Krenn, B. Lamprecht, and F. R. Aussenegg, Opt. Commun. **220**, 137 (2003).
- [20] A. V. Malyshev, V. A. Malyshev, and J. Knoester, Nano Letters **8**, 2369 (2008).
- [21] J. E. Halpert, J. R. Tischler, G. Nair, B. J. Walker, W. Liu, V. Bulović, and M. G. Bawendi, J. Phys. Chem. C **113**, 9986 (2009).
- [22] D. M. Eisele, J. Knoester, S. Kirstein, J. P. Rabe, and D. A. Vanden Bout, Nature Nanotechnology **4**, 658 (2009).
- [23] A. Eisfeld and J. S. Briggs, Phys. Rev. Lett. **96**, 113003 (2006).
- [24] M. Wewer and F. Stienkemeier, Phys. Chem. Chem. Phys. **7**, 1171 (2005).
- [25] H. Proehl, T. Dienel, R. Nitsche, and T. Fritz, Phys. Rev. Lett. **93**, 097403 (2004).
- [26] J. Seibt, A. Lohr, F. Würthner, and V. Engel, Phys. Chem. Chem. Phys. **9**, 6214 (2007).
- [27] R. L. Fulton and M. Gouterman, J. Chem. Phys. **35**, 1059 (1961).
- [28] B. Kopainsky, J. K. Hallermeier, and W. Kaiser, Chem. Phys. Lett. **83**, 498 (1981).
- [29] A. Eisfeld, L. Braun, W. T. Strunz, J. S. Briggs, J. Beck, and V. Engel, J. Chem. Phys. **122**, 134103 (2005).
- [30] J. Seibt, P. Marquetand, V. Engel, Z. Chen, V. Dehm, and F. Würthner, Chem. Phys. **328**, 354 (2006).
- [31] A. Eisfeld and J. S. Briggs, Chem. Phys. **324**, 376 (2006).
- [32] P. O. J. Scherer, Adv Mater **7**, 451 (1995).
- [33] F. C. Spano, Chem. Phys. Lett. **331**, 7 (2000).
- [34] A. Eisfeld and J. S. Briggs, Chem. Phys. Lett. **446**, 354 (2007).
- [35] J. Roden, A. Eisfeld, and J. S. Briggs, Chemical Physics **352**, 258 (2008).
- [36] J. Roden, A. Eisfeld, M. Dvořák, O. Bünermann, and F. Stienkemeier, J. Chem. Phys. submitted (2010).
- [37] J. Roden, A. Eisfeld, W. Wolff, and W. T. Strunz, Phys. Rev. Lett. **103**, 058301 (2009).
- [38] L. Diósi and W. T. Strunz, Phys. Lett. A **235**, 569 (1997).
- [39] T. Yu, L. Diosi, N. Gisin, and W. T. Strunz, Phys. Rev. A **60**, 91 (1999).
- [40] L. Diósi, N. Gisin, and W. T. Strunz, Phys. Rev. A **58**, 1699 (1998).
- [41] W. T. Strunz, L. Diósi, and N. Gisin, Phys. Rev. Lett. **82**, 1801 (1999).
- [42] A. Imamoglu, Phys. Rev. A **50**, 3650 (1994).
- [43] B. M. Garraway, Phys. Rev. A **55**, 2290 (1997).
- [44] L. Mazzola, S. Maniscalco, J. Piilo, K.-A. Suominen, and B. M. Garraway, Physical Review A (Atomic, Molecular, and Optical Physics) **80**, 012104 (pages 5) (2009).
- [45] A. Witkowski and W. Moffitt, J. Chem. Phys. **33**, 872 (1960).
- [46] R. E. Merrifield, Radiat. Res. **20**, 154 (1963).
- [47] R. L. Fulton and M. Gouterman, J. Chem. Phys. **41**, 2280 (1964).
- [48] A. Witkowski, in *Modern Quantum Chemistry III*, edited by Sinanoğlu (Academic Press, 1965), chap. III 3, pp. 161–175.
- [49] P. O. J. Scherer and S. F. Fischer, Chem. Phys. **86**, 269 (1984).
- [50] P. Walczak, A. Eisfeld, and J. S. Briggs, J. Chem. Phys. **128**, 044505 (2008).
- [51] V. May and O. Kühn, *Charge and Energy Transfer Dynamics in Molecular Systems* (WILEY-VCH, 2000).
- [52] V. Bargmann, Commun. Pure Appl. Math. **14**, 187 (1961).
- [53] W. T. Strunz and T. Yu, Phys. Rev. A **69**, 052115 (2004).
- [54] J. Bonča, S. A. Trugman, and I. Batistić, Phys. Rev. B **60**, 1633 (1999).
- [55] F. C. Spano, Journal of the American Chemical Society **131**, 4267 (2009).
- [56] J. Guthmuller, F. Zutterman, and B. Champagne, J. Chem. Theory Comput. **4**, 2094 (2008).
- [57] C. Meier and D. J. Tannor, J. Chem. Phys. **111**, 3365 (1999).
- [58] W. T. Simpson and D. L. Peterson, J. Chem. Phys. **26**, 588 (1957).
- [59] E. S. Medvedev and V. I. Osherov, *Radiationless Transitions in Polyatomic Molecules*, vol. 57 of *Springer Series in Chemical Physics* (Springer-Verlag, 1995).
- [60] E. W. Knapp, Chem. Phys. **85**, 73 (1984).
- [61] H. Fidler, J. Knoester, and D. A. Wiersma, J. Chem. Phys. **95**, 7880 (1991).
- [62] M. Schröder, U. Kleinekathöfer, and M. Schreiber, The Journal of Chemical Physics **124**, 084903 (pages 14) (2006).
- [63] A. Eisfeld, R. Kniprath, and J. Briggs, J. Chem. Phys. **126**, 104904 (2007).
- [64] I. Percival, *Quantum State Diffusion* (Cambridge University Press, 1998).
- [65] V. Engel, Chemical Physics Letters **189**, 76 (1992).
- [66] A. R. Bosco de Magalhães, C. H. d'Ávila Fonseca, and M. C. Nemes, Physica Scripta **74**, 472 (2006).
- [67] for the propagation we use a forth order Runge Kutta method.